



1 Shear rate effect on the residual strength characteristics of saturated loess

2 Baoqin Lian<sup>a,b</sup>, Jianbing Peng<sup>a\*</sup>, Qiangbing Huang<sup>a</sup>

3

4 <sup>a</sup>College of Geological Engineering and Surveying, Chang'an University, Key

5 Laboratory of Western China Mineral Resources and Geological Engineering, Xi'an

6 710054, China

7

8 <sup>b</sup>Department of Geology & Geophysics, Texas A&M University, College Station, TX

9 77843-3115, United States

10

11 \*Corresponding author: Jianbing Peng (dicexyl@gmail.com)

12

13

14

15

16



17 **Abstract**

18 Residual shear strength of soils is an important soil parameter for assessing the  
19 stability of landslides. To investigate the effect of the shear rate on the residual shear  
20 strength of loessic soils, a series of ring shear tests were carried out on loess from  
21 three landslides at two shear rates (0.1 mm/min and 1 mm/min). Naturally drained  
22 ring shear tests results showed that the shear displacement to achieve the residual  
23 stage for specimens with higher shear rate was greater than that of the lower rate; both  
24 the peak and residual friction coefficient became smaller with increase of shear rate  
25 for each sample; at two shear rates, the residual friction coefficients for all specimens  
26 under the lower normal stress were greater than that under the higher normal stress.  
27 The tests results revealed that the difference in the residual friction angle  $\phi_r$  at the two  
28 shear rates,  $\phi_r(1) - \phi_r(0.1)$ , under each normal stress level were either positive or  
29 negative values. However, the difference  $\phi_r(1) - \phi_r(0.1)$  under all normal stresses  
30 was negative, which indicates that the residual shear parameters reduced with the  
31 increasing of the shear rate in loess area. Such negative shear rate effect on loess  
32 could be attributed to a greater ability of clay particles in specimen to restore broken  
33 bonds at low shear rates.

34  
35 **Keywords:** Loess; Residual shear strength; Ring shear test; Shear rate; Residual shear  
36 parameter



37

## 38 **1. Introduction**

39 Residual shear strength of soil is of great significance for evaluating the stability  
40 for the slip surface of first-time landslides as well as reactivated landslides (Bishop et  
41 al., 1971; Mesri and Shahien, 2003). The residual strength of soils is defined as the  
42 minimum constant value of strength along the slip plane, in which the soil particles  
43 are reoriented and subjected to sufficiently large displacements in relatively low shear  
44 rate (Skempton, 1985).

45 Numerical studies have been done to assess the residual strength through the  
46 laboratory tests using ring shear tests and reversal direct shear tests (Moeyersons et al.,  
47 2008; Summa et al., 2010; Vithana et al., 2012; Chen and Liu, 2013; Summa et al.,  
48 2018). It is a generally accepted fact that the measurement of the residual strength is  
49 most preferred done with a ring shear test since it allows the soil specimen be sheared  
50 at unlimited displacement which can simulate the field conditions more accurately  
51 (Lupini et al., 1981; Sassa et al., 2004; Tiwari and Marui, 2005; Bhat, 2013). Until  
52 now, great efforts have been paid to the study of the shear rate effect on the minimum  
53 value of clay or sand strength at residual states (Morgenstern and Hungr, 1984; Lemos,  
54 1985; Tika, 1999; Tika and Hutchinson, 1999; Suzuki et al., 2007; Grelle and  
55 Guadagno, 2010; Bhat, 2013). As a result, the residual strength of clay or sand under  
56 the effect of shear rate has been made relatively clear. However, compared with the  
57 results of tests on clay or sand, understanding of the shear characteristics of silty soil,  
58 such as loess, is not yet complete. As pointed out by Ding (2016), some drained ring  
59 shear tests have concluded that the increase in shear rate causes the residual strength



60 of loess to increase. On the contrary, Kimura et al. (2014) reported that the residual  
61 strength of Malan loess decreases with the increase of shear rate. Furthermore, Wang  
62 et al. (2015) found that the effect of shear rate on residual strength of loess is closely  
63 associated with the normal stress levels, and the change in residual strength of loess  
64 samples under high normal stress levels is small in ring shear tests.

65 Therefore, some inconsistent or even opposite results have been reported in the  
66 ring shear tests on loess above, which implied that there is still a lack of experimental  
67 data on this topic. From the above investigations, it can be concluded that the effect of  
68 the shear rate on the residual strength of the loess is not fully understood and needs  
69 further scrutiny. Meanwhile, almost all of these investigations (Kimura et al., 2014;  
70 Wang et al., 2015; Ding, 2016) focused on the residual shear characteristics of loess  
71 obtained from the same location, while studies of loess collected from different  
72 locations have only been rarely performed. Moreover, it should be noted that the  
73 residual strength parameters (friction angle) obtained from using different shear rates  
74 may be adopted to provide a guide for designing some precision engineering which  
75 require high accuracy of the design parameters, thus, the effect of the shear rate on the  
76 residual strength of soils should be fully investigated to determine the parameters with  
77 high reliability. In addition, residual strength parameters of soil play a key role in  
78 assessing the stability analysis of landslides. Therefore, accurate determination of the  
79 residual strength parameters and their dependence on the shear rate may affect the  
80 stability evaluation of landslides. Thus, it is necessary to study the change of residual  
81 strength of loess with shear rate in order to have a good understanding of the suitable



82 approach for the residual strength parameters measurement.

83 In this backdrop, to clarify the residual shear characteristics of loess under the  
84 effect of the shear rate, a series of naturally drained ring shear tests were conducted on  
85 loess obtained from three landslides at two shear rates (0.1 mm/min and 1 mm/min).  
86 The residual shear characteristics of loess at the residual state was examined.  
87 Considering that shear strength of loess reduces with moisture content (Dijkstra et al.,  
88 1994; Zhang et al., 2009; Picarelli, 2010), ring shear tests were conducted on  
89 saturated loess samples corresponding to the worst condition in field engineering.  
90 Furthermore, this study investigated the change in the residual strength parameters of  
91 loess at different shear rates and their relationships with the normal stress in naturally  
92 drained ring shear tests as well.

93

## 94 **2. Geological setting of landslide sites**

95 Soil samples from three landslides in the northwest of China were selected in this  
96 study. Soil samples used for the ring shear tests and index measuring tests  
97 predominantly consist of loess deposits and were collected in a disturbed condition.  
98 For convenience, the names of landslide sites were abbreviated into Djg, Ydg, and  
99 Dbz. Fig. 1 shows the study sites and some views of the landslides.

### 100 **Dingjiagou landslide (Djg)**

101 The Djg landslide, located at the mouth of Dingjia Gully in Yan'an of China, is  
102 geologically composed of upper loess and lower sand shale in the Yan-chang  
103 formation. The dustpan-shaped landslide is inclined to the east, with its inclination  
104 75.85°. The landslide is 350 m in width, 180 m in length, 70 m in elevation. The



105 average thickness of slip mass is around 20 m, and the volume of landslide totaled  
106 approximately  $105 \times 10^4 \text{ m}^3$ . The slip mass is mainly constituted by loess, whereas the  
107 sliding bed consists of sand shale in Yan-chang formation. The thickness of the  
108 sliding zone varied from 30 to 50 cm. The front lateral region of the main slide  
109 section of the Djg landslide, where the sampling was performed, was found to be silty  
110 clay.

#### 111 **Yandonggou landslide (Ydg)**

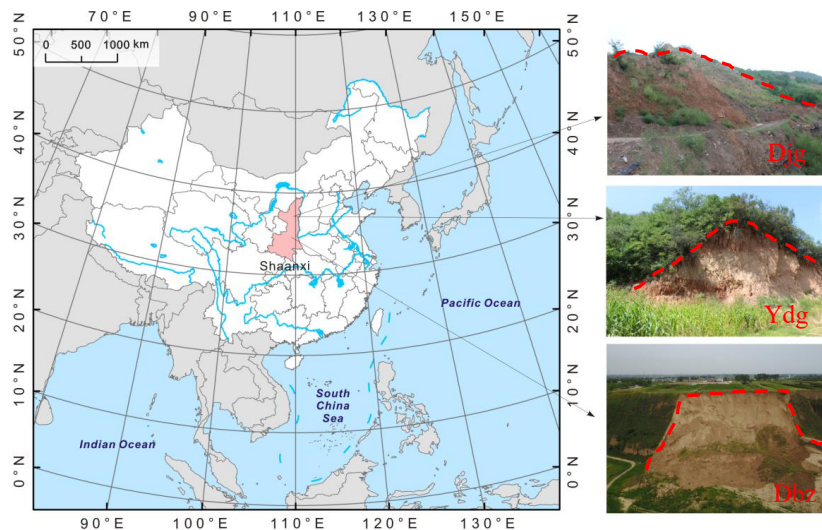
112 The Ydg landslide, located in the Qiaogou town of Yan'an in Shaan xi province of  
113 China. The top and the toe altitude of the landslide are about 1165 m and 1110 m  
114 above the sea level, with the height difference between the toe and the top of landslide  
115 about 55 m. The slides have well-developed boundaries with the main sliding  
116 direction of  $240^\circ$  and slope angle of  $30^\circ$ . From the landslides profile, the sliding  
117 masses from top to bottom were classified by late Pleistocene ( $Q_3$ ) loess, Lishi ( $Q_2$ )  
118 loess and clay soil, respectively. Multiple landslides had occurred in this site, and the  
119 soil samples used in this study were collected from  $Q_2$  loess stratum within the slide  
120 ranged from 4.5 m to 18 m in height.

#### 121 **Dabuzi landslide (Dbz)**

122 The Dbz landslide located in the middle part of Shaanxi province (about E  
123  $108^\circ 51' 36''$  and N  $34^\circ 28' 48''$ ), China, which is a semi-arid zone dominated by loessic  
124 geology. In this region, the investigated site is classified as a typical loess tableland  
125 with quaternary stratum. The sedimentary losses in this area are grey yellow, and the  
126 exposure stratum in this area has been divided into two stratigraphic units, namely,  
127 the upper Malan ( $Q_3$ ) loess and the lower Lishi ( $Q_2$ ) loess, of which the  $Q_3$  loess is



128 younger. The  $Q_3$  loess is closest to the surface and is up to approximately 12 m thick,  
129 while the thickness of  $Q_2$  loess may reach an upper limit of about 50 m (Leng et al.,  
130 2018). The loess in this area have well-developed vertical joints (Sun et al., 2009).  
131 The travel distance and the maximum width of the slip mass are roughly estimated to  
132 be 122 m and 133 m, respectively. The armchair-shaped landslide shows an apparent  
133 sliding plane, with an area of approximately 15,660 m<sup>2</sup> and about 66.25 m maximum  
134 difference in elevation. The main direction of this landslide is approximately 355°.  
135 The exposed side scarp of the landslide, where the sampling was done, was found to  
136 be entirely in the  $Q_2$  loess stratum.



137  
138 Figure 1. Location of study sites and some views of landslides

139 Notes: Red dashed lines in the Figure 1 represent landslide boundary.

### 140 3. Experimental scheme

#### 141 3.1. Testing sample

142 The fact that the residual shear strength is independent of the stress history has  
143 been reported by many researchers (Bishop et al., 1971; Stark Timothy et al., 2005;



144 Vithana et al., 2012). Thus, disturbed loess samples from each landslide weighing  
145 about 25 kg were collected to investigate the residual shear strength.

146 The soil samples were air-dried, and then crushed with a mortar and pestle. It was  
147 found that small lumps may exist in air-dried samples, which may be too big for the  
148 cell, so lumps were crushed in order to make sample uniform. This should be done  
149 with care so as not to destroy silty-dominated loess. After that, soil samples were  
150 processed through 0.5 mm sieve. Distilled water was then added to the soil samples  
151 until saturated water content were obtained. The physical parameters such as natural  
152 moisture content (*in-situ* moisture content), specific gravity, bulk density, plastic limit,  
153 and liquid limit were determined in accordance with the Chinese National Standards  
154 (CNS) GB/T 50123-1999 (standards for soil test methods) (SAC, 1999), but clay size  
155 was defined to be less than 2  $\mu\text{m}$  followed ASTM, D 422 (ASTM, 2007). Each soil  
156 sample was separated into clay (sub 0.002 mm), silt (0.002-0.075 mm), and sand  
157 (0.075-0.5 mm) fractions. The physical indexes of the soil are listed in Table 1.

158 The grain size distribution of soil was measured using a laser particle size  
159 analyzer Bettersize 2000 (Dandong Bettersize Instruments Corporation, Dandong,  
160 China). The sieved soil samples were used to determine particle size distribution. In  
161 this study, soil samples were treated with sodium hexaphosphate, serving as a  
162 dispersant, to disaggregate the bond between the particles. The results show that the  
163 clay fraction in Djg landslide soil (24%) is more than two times than that from Ydg  
164 (9%) and Dbz (9.1%). Furthermore, the particle size analysis illustrated that the  
165 percentage of silt-sized soil in three landslides ranged from 75.66% to 87.4%. In



166 addition, Ydg landslide soil consists of the greatest percentage of the sand fraction  
 167 which reaches up to 10.55%.

168 **Table 1** Physical parameters of slip-zone loess

sites	$\rho_d$	W	$\rho$	$G_S$	$W_L$	$W_p$	Grain size fractions (%)			
							<0.002mm	0.002-0.005mm	0.005-0.075	0.075-0.5mm
Djg	1.74	19.5	2.08	2.65	36	20	24	11.48	64.18	0.34
Ydg	1.47	18	1.74	2.71	33	19	9	5.28	75.17	10.55
Dbz	1.48	16	1.72	2.70	32	21	9.1	6.4	81	3.5

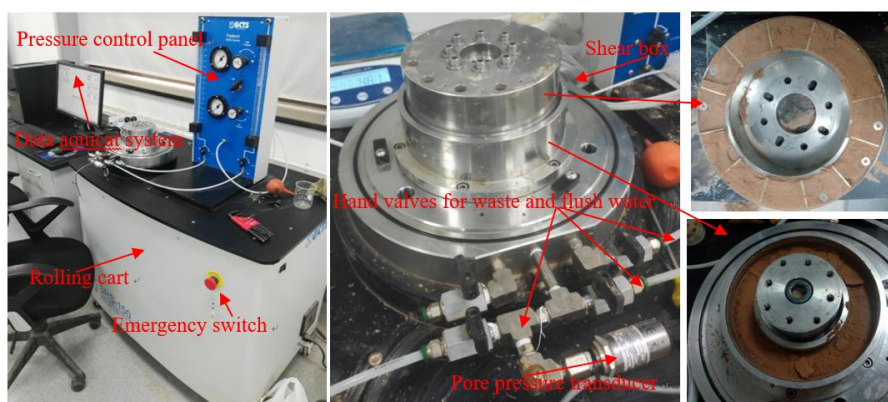
169 Notes:  $\rho_d$ = dry density ( $\text{g}/\text{cm}^3$ ); w=moisture water content (%);  $\rho$ = bulk density  
 170 ( $\text{g}/\text{cm}^3$ );  $G_S$  = specific gravity;  $W_L$ =liquid limit;  $W_p$ = plastic limit

171 **3.2. Testing apparatus**

172 An advanced ring shearing apparatus (SRS-150) manufactured by GCTS (Arizona,  
 173 USA) was adopted in ring shear tests and the photos of apparatus were shown in Fig.  
 174 2, which consists mainly of a shear box with an outer diameter of 150 mm, an inter  
 175 diameter of 100 mm and the maximal sample height of 250 mm. The shearing box  
 176 consists of the upper shear box and the lower shear box. In the shearing process, the  
 177 upper shear box keeps still while the lower one rotates. The apparatus which provides  
 178 effective specimen area of  $98 \text{ cm}^2$ , is capable of shearing the specimen for large  
 179 displacements. The annular specimen is confined by inside and outside metal rings.  
 180 Moreover, the specimen is confined by bottom annular porous plates and top annular  
 181 porous plates in which have sharp-edged radial metal fins which protrude vertically  
 182 into the top and bottom of the specimen at the shearing process. Two annual porous  
 183 plates were used to provide drainage condition in the test following previous research  
 184 (Stark and Vettel, 1992). The normal stress, shear strength and shear displacement can



185 be monitored by computer in shearing process. The measurement features of the ring  
186 shear apparatus employed in this study are described as follows: shear rate range from  
187 0.001 degrees to 360 degrees per minute, 10 kN axial load capacity, 300 N. m  
188 continuous torque capacity, maximum normal stress of 1000 kN/m<sup>2</sup>.



189  
190

Figure 2. Ring shear apparatus (SRS-150)

### 191 3.3. Testing procedure

192 In present study, reconstituted samples of the sub 0.5 mm soil fractions were used  
193 in the testing as it was reported that the residual strength of the soil was unaffected by  
194 its initial structure (Bishop et al., 1971; Vithana et al., 2012). Specimens were first  
195 prepared by adding distilled water to the air-dried soil until the saturated moisture  
196 contents were obtained. Then, specimens were kept in a sealed container for at least  
197 one week to fully hydrate. Afterwards, specimens are reconstituted in the ring-shaped  
198 chamber of the apparatus by compaction. The specimen was then consolidated under  
199 a specific effective normal stress in a range of 100 kN/m<sup>2</sup> to 400 kN/m<sup>2</sup> until  
200 consolidation was achieved. In this study, consolidation was completed when the  
201 consolidation deformation was smaller than 0.01 mm within 24 hr (Kramer et al.,  
202 1999; Shinohara and Golman, 2002). Then, the consolidated specimen is subjected to



203 shearing under constant normal stress by rotating the lower half of the shear box  
204 attached to a gear, while the upper half remains still. In ring shear tests, the normal  
205 stress at the shearing was the same as at consolidation stage. Shear strength of loess  
206 specimen was recorded at intervals of 1s before the peak shear strength, after the peak,  
207 the sampling rate was increased to 1 min.

208 In this study, ring shear tests were performed in a single stage under naturally  
209 drained condition and the samples were subjected to shear until the residual state was  
210 achieved. Drained condition of the shearing process is provided by two porous stones  
211 attached on the top and the bottom platen of the specimen container. As for soil  
212 specimens with low permeability, the rate of excess pore pressure generation in the  
213 shear box may exceeded that of pore-pressure dissipation, this type of condition is  
214 identified as naturally drained condition in previous studies(Okada et al., 2004).  
215 Furthermore, Tiwari (2000) asserted that it was acceptable to use a shear rate below  
216 1.1 mm/min to simulate the field naturally drained condition. Thus, shear rates of 0.1  
217 mm/min and 1 mm/min were used in this study to simulate the naturally drained  
218 condition of the slip zone soils.

#### 219 **4. Results**

220 Twenty -four specimens were tested to investigate the residual shear  
221 characteristics of the saturated loess in the ring shear apparatus. Residual shear  
222 strength of loess was determined following the research conducted by Bromhead  
223 (1992) who pointed out that the residual stage is attained if a constant shear stress is  
224 measured for more than half an hour. Tests results are shown in this section.



#### 225 **4.1. Shear behavior**

226 Figs. 3(a)- 5(a) show the typical shear characteristics of the loess (shear rate of 0.1  
227 mm/min and 1 mm/min) obtained from three different locations, where, the shear  
228 stress is plotted against the shear displacement. It is a widely accepted fact that  
229 normal stress has effect on the shear behavior of the soil (Stark Timothy et al., 2005;  
230 Eid, 2014; Kimura et al., 2015; Wang et al., 2019), thus, the shear behavior of  
231 samples at the peak and residual stages, where, the determined peak friction  
232 coefficient as well as residual friction coefficient are plotted in Figs. 3(b)-5(b) against  
233 the corresponding effective normal stresses as well. The friction coefficient is defined  
234 as the shear stress divided by the effective normal stress.

235 Figs. 3(a)-5(a) demonstrate that shear stress increases dramatically within small  
236 shear displacement and then reduces with shear displacement, until residual  
237 conditions were achieved at large displacements. Furthermore, it is obvious that the  
238 peak strength and the residual strength of samples with high shear rate are almost  
239 smaller than that of the samples with low shear rate. It can be found that shear  
240 displacement to achieve the residual stage for specimens with high shear rate is  
241 greater than that of the low rate. For example, the minimum shear displacements for  
242 attaining residual condition for Djg specimens with low and high shear rate were  
243 about 360 mm and 650 mm, respectively. Under the shear rate of 0.1 mm/min and 1  
244 mm/min, Ydg specimens need approximately 80 mm and 1,400 mm displacement to  
245 achieve residual stage. However, Dbz specimens require about 40 mm and 60 mm  
246 displacement to reach residual condition for low and high shear rate, respectively.



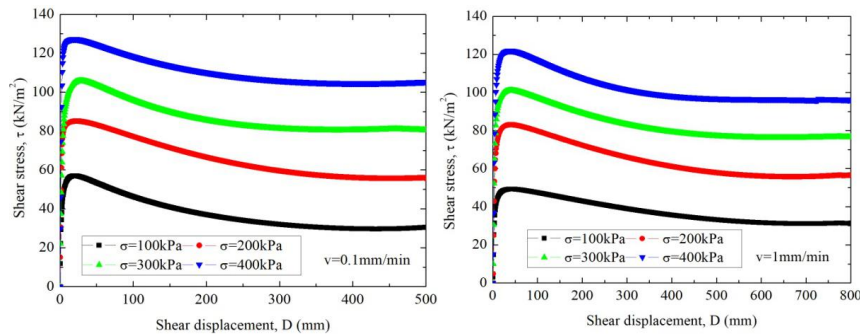
247 In Figs. 3(a)- 5(a), a clear drop can be seen, at any normal stress, for specimens  
248 obtained from all sites. It is obvious that Djg specimens showed greater peak-post  
249 drop than that of Ydg and Dbz specimens. For example, at the normal stress of 100  
250 kN/m<sup>2</sup>, Djg samples show approximately 47.3% and 36.8% decrease from the peak  
251 friction coefficient to the residual friction coefficient at low and high shear rates (Fig.  
252 3(b)), respectively, which is greater than in the Ydg samples (about 9.8% and 10.3%  
253 in Fig. 4(b)) and Dbz samples (about 2.4% and 3.2% in Fig. 5(b)). In Djg samples, an  
254 obvious slickenside was observed on the shear surface (Fig. 6). This phenomenon  
255 indicates a high degree of reorientation of platy clay minerals parallel to the direction  
256 of shearing. In Figs. 3(b)- 5(b), on average, it was found that the decrease in the  
257 friction coefficient from the peak strength in the Djg sample is almost 18.1% and  
258 21.3% for the sample consolidated at normal stress of 400 kN/m<sup>2</sup> under the low and  
259 high shear rate (Fig. 3(b)), while such reduction in friction coefficient in Ydg sample  
260 are only about 4.1% and 4.8% (Fig. 4(b)). Furthermore, under the low and high shear  
261 rate, the friction coefficient reduction in Dbz samples are only approximately 5.6%  
262 and 6.0% (Fig. 5(b)). Skempton (1985) reported that the strength of soils falls to the  
263 residual value in ring shear tests, owing to reorientation of platy clay minerals parallel  
264 to the direction of shearing. Based on the conclusion that the post-peak drop in  
265 strength of normally consolidated soil is only due to particle reorientation after the  
266 peak strength (Skempton, 1964; Mesri and Shahien, 2003), the results demonstrated  
267 that the Djg landslide soil existed the greater particle reorientation compared with that  
268 of other two landslide soils.



269

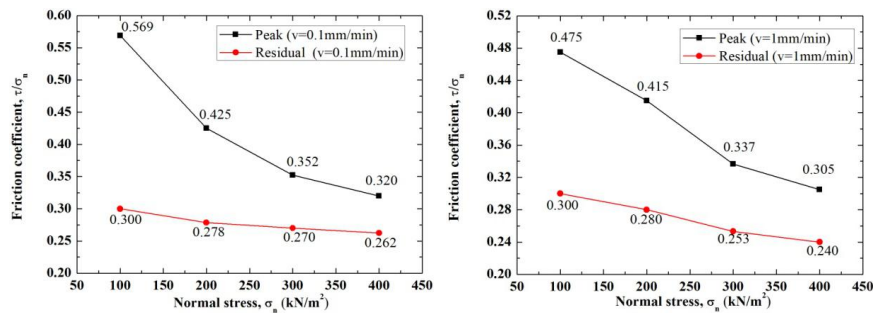
270 **4.2. Effect of normal stress on the friction coefficients**

271 It can be seen from the Figs. 3(b)-5(b) that the friction coefficients (peak and  
 272 residual) are higher at low effective normal stress levels compared with that at high  
 273 normal stress. For example, with normal stress increasing from 100 kN/m<sup>2</sup> to 400  
 274 kN/m<sup>2</sup>, the peak and residual friction coefficient of Djg landslide soils at the shear  
 275 rate of 0.1 mm/min reduce from 0.569 to 0.32 and from 0.3 to 0.262 (Fig. 3(b)),  
 276 respectively. Similarly, results obtained from other two landslides loess also show that  
 277 the friction coefficients decrease nonlinearly with normal stresses (Figs. 4(b) and  
 278 5(b)). Furthermore, specimens with shear rate of 0.1 mm/min attained greater friction  
 279 coefficients than that with shear rate of 1 mm/min (Figs. 3(b)-5(b)).



280

281 (a) Relationship between shear stress and shear displacement



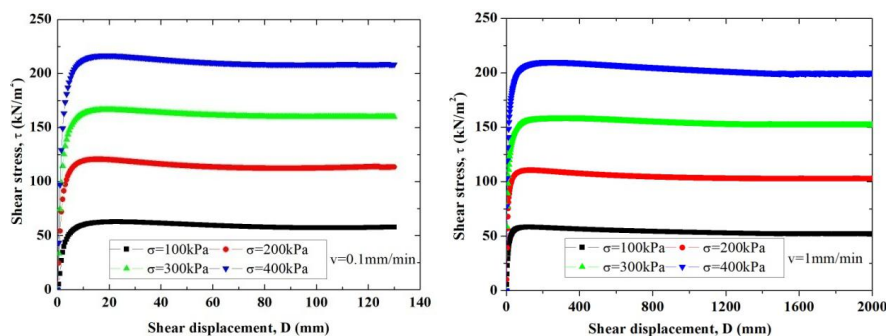
282

283 (b) Relationship between friction coefficient and normal stress



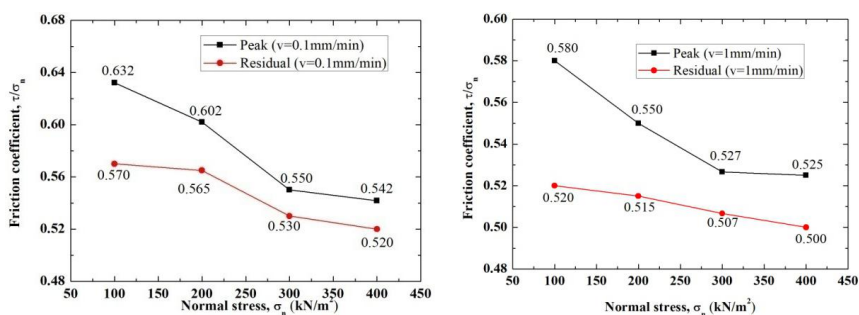
284 Figure 3. Shear behavior characteristics of D<sub>1</sub>g soil samples

285



286

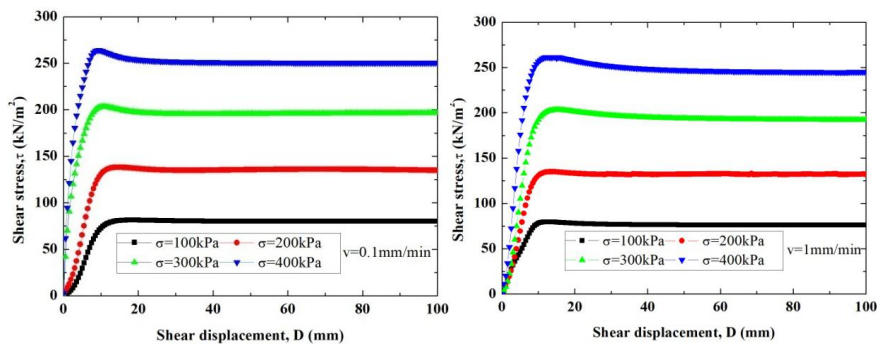
287 (a) Relationship between shear stress and shear displacement



288

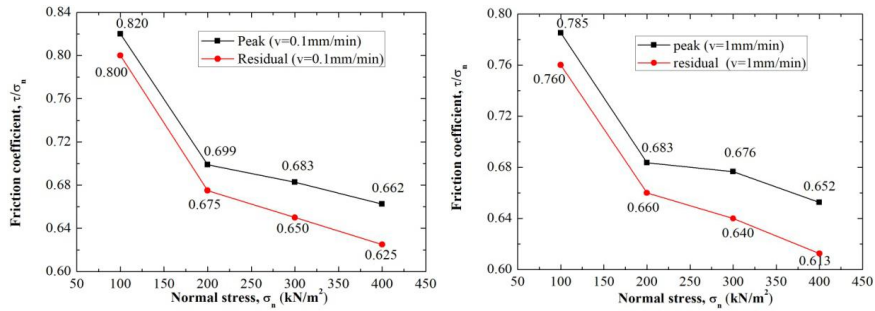
289 (b) Relationship between friction coefficient and normal stress

290 Figure 4. Shear behavior characteristics of Y<sub>d</sub>g soil samples



291

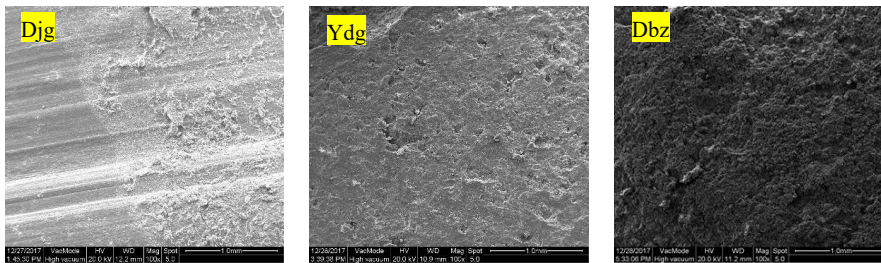
292 (a) Relationship between shear stress and shear displacement



293

294 (b) Relationship between friction coefficient and normal stress

295 Figure 5. Shear behavior characteristics of the Dbz soil samples



296

297 Figure 6. SEM photographs of the shear surface of loess samples (100 magnification)

298 **4.3. Effects of shear rate on residual strength parameter**

299 For the samples described above, Figs. 7-9 show the relationships between the

300 residual friction coefficient and the normal stress, and the residual strength parameters.

301 The residual friction coefficient is plotted against the normal stress. The residual

302 friction coefficient is defined as the residual shear strength divided by normal stress. It

303 has been recognized that the shear strength parameters including cohesion and friction

304 angle (Terzaghi, 1951; Stark Timothy et al., 2005). However, according to the

305 previous studies, the residual angle of soils varies depended on the soil properties as

306 well as the magnitude of normal stress provided the residual cohesion of soil is zero

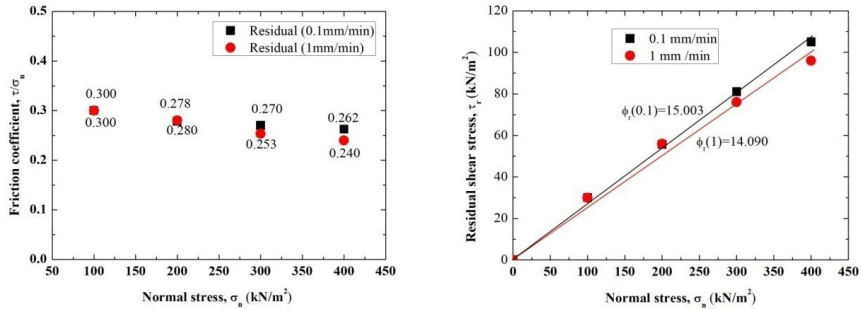
307 (Skempton, 1964; Bishop; Kimura et al., 2014). Thus, in this study, the residual

308 frictions are calculated by Coulomb's law assumed the residual cohesion is zero



309 following the previous studies (Skempton, 1985). The residual strength parameters  
310 were defined as  $\phi_r(0.1)$  and  $\phi_r(1)$  at the low shear rate and high shear rate,  
311 respectively. And the difference between the residual friction angles at two shear rates  
312 was defined as  $\phi_r(1) - \phi_r(0.1)$ . Comparatively, the residual friction coefficient was  
313 defined as  $\tau_r/\sigma_n(0.1)$  at the low shear rate and  $\tau_r/\sigma_n(1)$  at the high shear rate,  
314 respectively. Furthermore, the difference between the residual friction coefficients  
315 was defined as  $\tau_r/\sigma_n(1) - \tau_r/\sigma_n(0.1)$ . Table 2 summarized the residual shear  
316 parameters of the landslide soils.

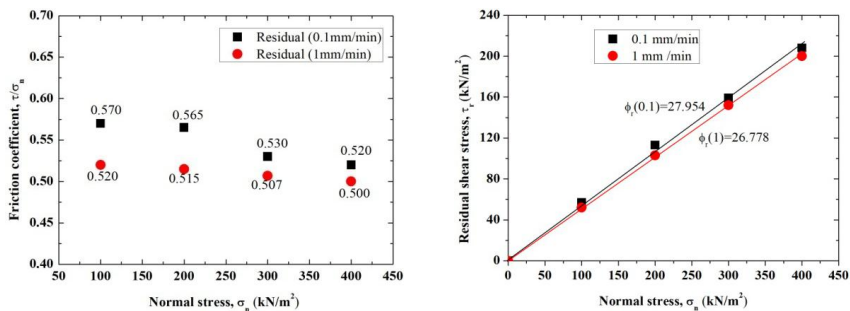
317 Fig. 7 shows that the residual friction coefficients are relatively low in Djg  
318 samples. The coefficients  $\tau_r/\sigma_n(0.1)$  and  $\tau_r/\sigma_n(1)$  at the normal stress of 100 kN/m<sup>2</sup>  
319 to 400 kN/m<sup>2</sup> ranged from 0.3 to 0.262 and from 0.3 to 0.24, respectively. The  
320 difference between the friction coefficients,  $\tau_r/\sigma_n(1) - \tau_r/\sigma_n(0.1)$ , at each normal  
321 stress level are varied in a range of -0.022 to +0.002. For the difference between the  
322 residual friction angles,  $\phi_r(1) - \phi_r(0.1)$ , ranged from -1.212° to +0.079° (Table 2). For  
323 normal stress above 200 kN/m<sup>2</sup>, the residual friction coefficient  $\tau_r/\sigma_n(0.1)$  was found  
324 to be greater than the residual friction coefficient  $\tau_r/\sigma_n(1)$ . For this sample, residual  
325 friction coefficients show a slight decrease with the shear rate for normal stress above  
326 200 kN/m<sup>2</sup>.



327

328 Figure 7. Relationships between residual shear stress and normal stress, and  
 329 residual strength parameter for Djg soil sample

330 Fig. 8 gives the results of the Ydg samples. The coefficients  $\tau_r/\sigma_n(0.1)$  and  $\tau_r/\sigma_n$   
 331 (1) under the normal stress of 100 kN/m<sup>2</sup> to 400 kN/m<sup>2</sup> ranged from 0.57 to 0.52 and  
 332 from 0.52 to 0.50, respectively. Furthermore, the difference  $\tau_r/\sigma_n(1) - \tau_r/\sigma_n(0.1)$  at  
 333 each normal stress was from -0.05 to -0.02. As for the difference between the residual  
 334 friction angles,  $\phi_r(1) - \phi_r(0.1)$ , was in a range of -2.218° to -0.909°. In case of Ydg  
 335 soil sample, the residual friction coefficients decreased with increase of shear rate for  
 336 all normal stress levels.



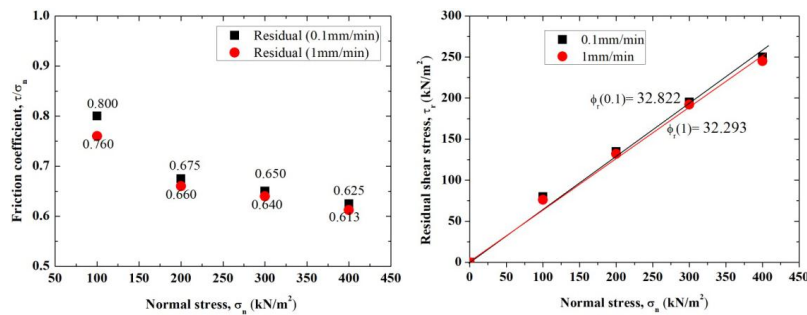
337

338 Figure 8. Relationships between residual shear stress and normal stress, and residual  
 339 strength parameter for Ydg soil samples

340 Fig. 9 presents the results of the Dbz samples. The coefficients  $\tau_r/\sigma_n(0.1)$  and  $\tau_r/\sigma_n$   
 341 (1) at the normal stress of 100 kN/m<sup>2</sup> to 400 kN/m<sup>2</sup> ranged from 0.8 to 0.625 and



342 from 0.76 to 0.613, respectively. The difference  $\tau_r/\sigma_n(1) - \tau_r/\sigma_n(0.1)$  at each normal  
 343 stress was from -0.04 to -0.01. The difference  $\phi_r(1) - \phi_r(0.1)$  was from  $-1.425^\circ$  to  
 344  $-0.405^\circ$ . For Dbz samples, there was somewhat decrease tendency of the residual  
 345 friction coefficients with the increasing of the shear rate for all normal stress levels. It  
 346 is noted that the maximum difference was found at the lowest normal stress of 100  
 347  $\text{kN/m}^2$ .



348  
 349 Figure 9. Relationships between residual shear stress and normal stress, and residual  
 350 strength parameter for Dbz soil sample

351 Table 2 summarizes residual strength parameters including  $\phi_r(0.1)$  and  $\phi_r(1)$  of  
 352 all specimens obtained from the ring shear tests in this study. As for the Djg samples,  
 353 the residual strength parameter  $\phi_r(0.1)$  and  $\phi_r(1)$  for all normal stress were found to  
 354 be  $15.003^\circ$  and  $14.09^\circ$  (Fig. 7), respectively. However, the residual friction angles  $\phi_r$   
 355  $(0.1)$  and  $\phi_r(1)$  of the Ydg samples were obtained to be  $27.954^\circ$  and  $26.778^\circ$  (Fig. 8),  
 356 respectively. In the case of Dbz sample, the friction angles  $\phi_r(0.1)$  and  $\phi_r(1)$  were  
 357 high,  $32.822^\circ$  and  $32.293^\circ$  (Fig. 9), respectively. The residual friction angles  $\phi_r(0.1)$   
 358 and  $\phi_r(1)$  under all normal stresses were from  $15.003^\circ$  to  $32.822^\circ$  and from  $14.09^\circ$  to  
 359  $32.293^\circ$ , respectively.

360 Due to the influence of the shear rate, the difference  $\phi_r(1) - \phi_r(0.1)$  in the Djg,



361 Ydg and Dbz samples, were  $-0.913^\circ$ ,  $-1.176^\circ$  and  $-0.529^\circ$ , respectively. Wang (2014)  
 362 and Fan et al. (2017) asserted that the residual shear strength of remolded loess hardly  
 363 affected by shear rate below 5 mm/min. However, the results in this study shown that  
 364  $\phi_r(1) - \phi_r(0.1)$  under all normal stress levels were negative for loess. Moreover, the  
 365 absolute value of  $\phi_r(1) - \phi_r(0.1)$  in Ydg samples even reached up to  $1.176^\circ$ .

366

367 Table 2 Residual shear strength parameter of landslide soils

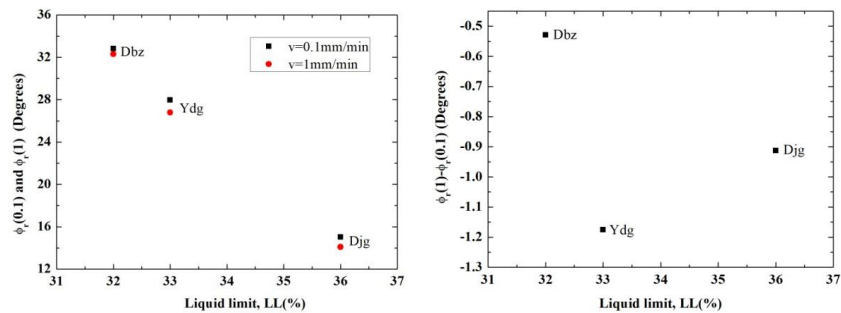
No	Sample	Normal stress(kN/m <sup>2</sup> )	Residual strength parameter				Difference in parameter	
			0.1 mm/min $\phi_r(0.1)$ ( $c_r(0.1)=0$ )		1 mm/min $\phi_r(1)$ ( $c_r(1)=0$ )		$\phi_r(1) - \phi_r(0.1)$ (Degrees)	
			(Degrees)		(Degrees)			
		Under each $\sigma_n$	Under all $\sigma_n$	Under each $\sigma_n$	Under all $\sigma_n$	Under each $\sigma_n$	Under all $\sigma_n$	
1	Djg	100	16.699	15.003	16.699	14.090	0	-0.913
		200	15.563		15.642		0.079	
		300	15.110		14.216		-0.894	
		400	14.708		13.496		-1.212	
2	Ydg	100	29.683	27.954	27.474	26.778	-2.209	-1.176
		200	29.466		27.248		-2.218	
		300	27.923		26.870		-1.053	
		400	27.474		26.565		-0.909	
3	Dbz	100	38.660	32.822	37.235	32.293	-1.425	-0.529
		200	34.019		33.425		-0.594	
		300	33.024		32.619		-0.405	
		400	32.005		31.487		-0.518	

368

369 **4.4. Influence of the shear rate on the residual friction angles according to soil**  
 370 **properties**



371 It has been recognized that residual shear strength of soils is closely related with  
372 soil properties, such as particle size distribution (PSD), liquid limit (LL), plasticity  
373 index ( $I_p$ ) and clay fraction (CF) (Terzaghi et al., 1996). Fig. 10 depicts the  
374 relationships between residual friction angles as well as the difference in the residual  
375 friction angles and soil properties including liquid limit (LL), plasticity index ( $I_p$ ) and  
376 clay fraction (CF) at two shear rates. The residual friction angles at two shear rates  
377 decreased nonlinearly with the increasing of the LL. As for the relationship between  
378 the  $\phi_r$  and  $I_p$ , the  $\phi_r$  under the low and high shear rates decreases from about  $32^\circ$  to  $15^\circ$   
379 with increasing the  $I_p$  from 11 to 16. These findings agree well with the early studies  
380 (Wesley, 2003; Tiwari et al., 2005). With increasing of CF from 9% to 24%, the  
381 residual friction angles under low and high shear rates were found to decrease (Fig.  
382 10). These observations are consistent with previous studies (Lupini et al., 1981; Gibo  
383 et al., 1987). Interestingly, for Dbz and Ydg soils of which have similar percentage of  
384 clay fraction, the residual friction angles at both shear rates varied. However, in the  
385 relationships between the difference in the residual friction angles and the soil  
386 properties, no clear correlations were found.



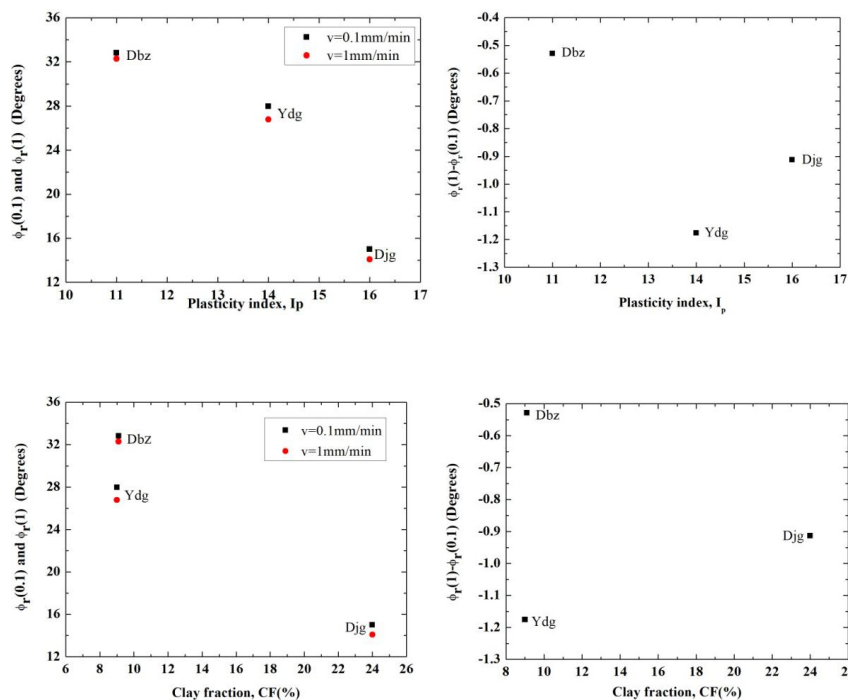
387

388



389

390



391

392 Figure 10. Relationships between residual shear parameter, the difference in  
393 residual shear parameter and the soil properties at two shear rates

## 394 5. Discussion

395 Examination of the ring shear test results provides a basis for some general  
396 comments on the use of tests results with different shear rates, partially deepening  
397 some aspects deriving from previous studies.

398 From the experimental results on the three selected landslides, it was found that  
399 there is a negative relationship between residual friction coefficients and shear rates  
400 for all samples (Figs. 7, 8 and 9). Such a negative effect of shear rate (higher residual  
401 friction coefficients at lower rates) has been reported in the literature for fine-grained  
402 soils (Tika et al., 1996; Gratchev Ivan and Sassa, 2015). This effect may be closely  
403 associated with ability of clay particles in specimen to restore broken bonds at



404 different shear rates. Previous studies (Osipov et al., 1984; Perret et al., 1996).  
405 concluded that with higher shear rates, the breakdown of the bonds between clay  
406 particles or flocs exceeds the restoration bond, leading to reduction in residual friction  
407 coefficients. In contrast, the bonds between particles are rebuilt quickly and the  
408 recovery rate can catch up the breakdown rate at lower shear rates. Therefore, the  
409 weaker bonding between particles could explain the strength drop with the increasing  
410 of the shear rate in this study.

411 The difference between the friction coefficients,  $\tau_r/\sigma_n(1) - \tau_r/\sigma_n(0.1)$ , at each  
412 normal stress level varies in different locations.  $\tau_r/\sigma_n(1) - \tau_r/\sigma_n(0.1)$  in Ydg specimen  
413 are greater compared with that in Djg and in Dbz specimen (Table 2). As for Ydg and  
414 Dbz specimen, it is found that the shear rate effect on the friction coefficient can be  
415 seen to decrease with normal stress (Figs. 8 and 9). By contrast, there is an increasing  
416 tendency in the influence of shear rate on the friction coefficient with normal stress in  
417 Djg specimen (Fig. 7). Gibo et al. (1987) reported that the residual friction angle of  
418 soils was controlled by the effective normal stress as well as by the CF. Interestingly,  
419 Ydg (with CF 9%) and Dbz (with CF 9.1%) specimens with almost the same fraction  
420 of clay showed similar shear rate effect on the residual friction coefficient with  
421 normal stress increasing, however, Djg (with 24% CF) showed the contrast tendency  
422 of shear rate effect on residual friction coefficient with normal stress, indicating that  
423 such effect is closely associated with CF. Therefore, as for Ydg and Dbz with  
424 relatively low fraction of CF, there is an increase effect of shear rate on residual  
425 friction coefficient with decreasing of normal stress. Thus, for the application of



426 measured residual friction coefficient for stability analysis of shallow landslides with  
427 lower overburden pressure, it is significant for us to use a low shear rate in ring shear  
428 tests to measure residual shear strength parameters. On other hand, for Djg with high  
429 CF, it is more reliable to use a low shear rate in ring shear tests to determine residual  
430 friction coefficient for stability analysis of deep landslides with high overburden  
431 pressure.

432

## 433 **6. Conclusion**

434 A series of ring shear tests were conducted on loess obtained from three landslides  
435 to study the residual shear characteristics of saturated loess. Based on the test results,  
436 the effect of the shear rate on the residual shear characteristics of loess in naturally  
437 drained condition was examined. The following conclusions can be drawn:

- 438 1. Ring shear test revealed that (i) shear displacement to achieve the residual stage  
439 with high shear rate is greater than that of the low shear rate; (ii) Both the peak  
440 and residual friction coefficient became smaller with increase of shear rate for  
441 each sample; (iii) The greater difference between the peak and the residual friction  
442 coefficient in loess samples could be attributed to relatively well-developed  
443 slickenside on the shear surface.
- 444 2. At the two shear rates, there was a nonlinearly decrease trend of the residual  
445 friction coefficient with the normal stress in all loess samples. The difference  
446 between the friction coefficients,  $\tau_r/\sigma_n(1) - \tau_r/\sigma_n(0.1)$  was found to decrease  
447 with normal stress in Ydg and Dbz specimens while increase with normal stress in



448 D<sub>rg</sub> specimens, indicating that CF may be closely associated with shear rate effect  
449 on residual friction coefficient with normal stress.

450 3. The difference at the two shear rates,  $\phi_r(1) - \phi_r(0.1)$ , under each normal stress  
451 level were either negative or positive. However, under all normal stress, the  
452 difference at the two shear rates  $\phi_r(1) - \phi_r(0.1)$  was found to be negative. Such  
453 negative shear rate effect on loess could be attributed to greater ability of clay  
454 particles in specimen to restore broken bonds at low shear rates.

455 4. The relationships between the  $\phi_r$  under two shear rates and soil properties (LL, I<sub>p</sub>),  
456 demonstrated that the  $\phi_r$  at both shear rates decreased gradually with the  
457 increasing of LL and I<sub>p</sub>. However, no clear correlations between the difference in  
458 the  $\phi_r$  at low and high shear rates and the soil properties were found.

459

460



461 **Code availability:** Code can be made available by the authors upon request.

462 **Data availability:** Data can be made available by the authors upon request.

463 **Author contributions:** BL,JP and QH conceived and designed the method; BL  
464 produced the results, and wrote the original manuscript under the supervision of JP.  
465 JP and QH writing-review and editing.

466 **Competing interest:** The authors declare that they have no conflicts of interest.

467 **Acknowledgments:** This research was supported by the Major Program of National  
468 Natural Science Foundation of China (Grant No. 41790440), the National Natural  
469 Science Foundation of China (No.41902268) and the China Postdoctoral Science  
470 Foundation (No. 2019T120871).



## 471 **References**

- 472 ASTM: (D422)Standard test method for particle-size analysis of soils. 2007.
- 473 Bhat, D. R.: Effect of shearing rate on residual strength of kaolin clay, PhD, Graduate school of Science  
474 and Engineering, Ehime University, Japan, 2013.
- 475 Bishop, A. W.: Shear strength parameters for undisturbed and remoulded specimens., Foulis and Co,  
476 3–58, 1971.
- 477 Bishop, A. W., Green, G. E., Garga, V. K., Andresen, A., and Brown, J. D.: A new ring shear apparatus  
478 and its application to the measurement of residual strength, *Geotechnique*, 21, 273-328, 1971.
- 479 Bromhead, E.: The stability of slopes, blackie academic and professional, London. UK, 1992. 1992.
- 480 Chen, X. P. and Liu, D.: Residual strength of slip zone soils, *Landslides*, 11, 305-314, 2013.
- 481 Dijkstra, T., Rogers, C., Smalley, I., Derbyshire, E., Li, Y. J., and Meng, X. M.: The loess of north-central  
482 China: geotechnical properties and their relation to slope stability, *Engineering Geology*, 36, 153-171,  
483 1994.
- 484 Ding, H.: Ring shear tests on strength properties of loess in different regions. (In Chinese), Master,  
485 Northwest A&F University, 2016.
- 486 Eid, H. T.: Stability charts for uniform slopes in soils with nonlinear failure envelopes, *Engineering  
487 Geology*, 168, 38-45, 2014.
- 488 Fan, X., Xu, Q., Scaringi, G., Li, S., and Peng, D.: A chemo-mechanical insight into the failure mechanism  
489 of frequently occurred landslides in the Loess Plateau, Gansu Province, China, *Engineering Geology*,  
490 228, 337-345, 2017.
- 491 Gibo, S., gashira, K., and Ohtsubo, M.: Residual strength of smectite-dominated soils from the  
492 Kamenose landslide in Japan, *Can Geotech J*, 24, 456–462, 1987.
- 493 Gratchev Ivan, B. and Sassa, K.: Shear strength of clay at different shear rates, *Journal of Geotechnical  
494 and Geoenvironmental Engineering*, 141, 2015.
- 495 Grelle, G. and Guadagno, F. M.: Shear mechanisms and viscoplastic effects during impulsive shearing,  
496 *Géotechnique* 41, 60, 91–103, 2010.
- 497 Kimura, S., Nakamura, S., and Vithana, S. B.: Influence of effective normal stress in the measurement  
498 of fully softened strength in different origin landslide soils, *Soil Till Res*, 145, 47-54, 2015.
- 499 Kimura, S., Nakamura, S., Vithana, S. B., and Sakai, K.: Shearing rate effect on residual strength of  
500 landslide soils in the slow rate range, *Landslides*, 11, 969-979, 2014.
- 501 Kramer, S., Wang, C., and Byers, M.: Experimental measurement of the residual strength of particulate  
502 materials, *Physics and mechanics of soil liquefaction*, 1999. 249-260, 1999.
- 503 Lemos, L.: Earthquake loading of shear surfaces in slopes, *Proc.11th I.C.S.M.F.E.*, 4, 1955-1958, 1985.
- 504 Leng, Y., Peng, J., Wang, Q., Meng, Z., and Huang, W.: A fluidized landslide occurred in the Loess  
505 Plateau: A study on loess landslide in South Jingyang tableland, *Engineering Geology*, 236, 129-136,  
506 2018.
- 507 Lupini, J. F., Skinner, A. E., and Vaughan, P. R.: The drained residual strength of cohesive soils,  
508 *Geotechnique*, 31, 181-213, 1981.
- 509 Mesri, G. and Shahien, M.: Residual shear strength mobilized in first-time slope failures, *Journal of  
510 Geotechnical and Geoenvironmental Engineering*, 129, 12-31, 2003.
- 511 Moeyersons, J., Van Den Eeckhaut, M., Nyssen, J., Gebreyohannes, T., Van de Wauw, J., Hofmeister, J.,  
512 Poesen, J., Deckers, J., and Mitiku, H.: Mass movement mapping for geomorphological understanding  
513 and sustainable development: Tigray, Ethiopia, *Catena*, 75, 45-54, 2008.



- 514 Morgenstern, N. R. and Hungr, O.: High Velocity ring shear tests on sand, *Geotechnique*, 34, 415-421,  
515 1984.
- 516 Okada, Y., Sassa, K., and Fukuoka, H.: Excess pore pressure and grain crushing of sands by means of  
517 undrained and naturally drained ring-shear tests, *Engineering Geology*, 75, 325-343, 2004.
- 518 Osipov, V., Nikolaeva, S., and Sokolov, V.: Microstructural changes associated with thixotropic  
519 phenomena in clay soils, *Geotechnique*, 34, 293-303, 1984.
- 520 Perret, D., Locat, J., and Martignoni, P.: Thixotropic behavior during shear of a fine-grained mud from  
521 Eastern Canada, *Engineering Geology*, 43, 31-44, 1996.
- 522 Picarelli, L.: Discussion on "A rapid loess flowslide triggered by irrigation in China" by D. Zhang, G.  
523 Wang, C. Luo, J. Chen, and Y. Zhou, *Landslides*, 7, 203-205, 2010.
- 524 SAC: Standardization Administration of China (SAC), Ministry of Construction, Ministry of Water  
525 Resources. In: China National Standards GB/T50123-1999: Standard for Soil Test Method, China  
526 Planning Press, Beijing, 1999.
- 527 Sassa, K., Fukuoka, H., Wang, G., and Ishikawa, N.: Undrained dynamic-loading ring-shear apparatus  
528 and its application to landslide dynamics, *Landslides*, 1, 7-19, 2004.
- 529 Shinohara, K. and Golman, B.: Dynamic shear properties of particle mixture by rotational shear test,  
530 *Powder Technol*, 122, 255-258, 2002.
- 531 Skempton, A. W.: Long-term stability of clay slopes, *Geotechnique*, 14, 77-102, 1964.
- 532 Skempton, A. W.: Residual strength of clays in landslides, folded strata and the laboratory,  
533 *Geotechnique*, 35, 3-18, 1985.
- 534 Skempton: Long-term stability of clay slopes, *Geotechnique*, 14, 77-102, 1964.
- 535 Stark, T. D. and Vettel, J. J.: Bromhead ring shear test procedure, *Geotech Test J*, 15, 24-32, 1992.
- 536 Stark Timothy, D., Choi, H., and McCone, S.: Drained shear strength parameters for analysis of  
537 landslides, *Journal of Geotechnical and Geoenvironmental Engineering*, 131, 575-588, 2005.
- 538 Summa, V., Margiotta, S., Medici, L., and Tateo, F.: Compositional characterization of fine sediments  
539 and circulating waters of landslides in the southern Apennines–Italy, *Catena*, 171, 199-211, 2018.
- 540 Summa, V., Tateo, F., Giannossi, M., and Bonelli, C.: Influence of clay mineralogy on the stability of a  
541 landslide in Plio-Pleistocene clay sediments near Grassano (Southern Italy), *Catena*, 80, 75-85, 2010.
- 542 Sun, P., Peng, J.-b., Chen, L.-w., Yin, Y.-p., and Wu, S.-r.: Weak tensile characteristics of loess in China —  
543 An important reason for ground fissures, *Engineering Geology*, 108, 153-159, 2009.
- 544 Suzuki, M., Tsuzuki, S., and Yamamoto, T.: Residual strength characteristics of naturally and artificially  
545 cemented clays in reversal direct box shear test, *Soils And Foundations*, 47, 1029-1044, 2007.
- 546 Terzaghi, K.: *Theoretical soil mechanics*, Chapman And Hall, Limited.; London, 1951.
- 547 Terzaghi, K., Peck, R. B., and Mesri, G.: *Soil mechanics in engineering practice*, John Wiley & Sons,  
548 1996.
- 549 Tika, T.: Ring shear tests on a carbonate sandy silt, *Geotechnical Testing Journal*, 22, 1999.
- 550 Tika, T. E. and Hutchinson, J. N.: Ring shear tests on soil from the Vaiont landslide slip surface,  
551 *Geotechnique*, 49, 59-74, 1999.
- 552 Tika, T. E., Vaughan, P. R., and Lemos, L. J. L. J.: Fast shearing of pre-existing shear zones in soil,  
553 *Geotechnique*, 46, 197-233, 1996.
- 554 Tiwari, B.: Analysis of landslide mechanism of Okimi Landslide, M. Sc. Thesis, Niigata University, 2000.  
555 2000.
- 556 Tiwari, B., Brandon, T. L., Marui, H., and Tuladhar, G. R.: Comparison of residual shear strengths from  
557 back analysis and ring shear tests on undisturbed and remolded specimens, *Journal of Geotechnical*



558 and Geoenvironmental Engineering, 131, 1071-1079, 2005.  
559 Tiwari, B. and Marui, H.: A new method for the correlation of residual shear strength of the soil with  
560 mineralogical composition, Journal of Geotechnical and Geoenvironmental Engineering, 131,  
561 1139-1150, 2005.  
562 Vithana, S. B., Nakamura, S., Kimura, S., and Gibo, S.: Effects of overconsolidation ratios on the shear  
563 strength of remoulded slip surface soils in ring shear, Engineering Geology, 131-132, 29-36, 2012.  
564 Wang, J.-D., Li, P., Ma, Y., and Vanapalli, S. K.: Evolution of pore-size distribution of intact loess and  
565 remolded loess due to consolidation, Journal of Soils and Sediments, 19, 1226-1238, 2019.  
566 Wang, S., Wu, W., Xiang, W., and Liu, Q.: Shear behaviors of saturated loess in naturally drained  
567 ring-shear tests. In: Recent Advances in Modeling Landslides and Debris Flows, Springer, 2015.  
568 Wang, W.: Residual Strength of Remolded Loess in Ring Shear Tests., PhD Northwest A & F University  
569 of China, 2014.  
570 Wesley, L. D.: Residual strength of clays and correlations using atterberg limits, Geotechnique, 23,  
571 669-672, 2003.  
572 Zhang, D., Wang, G., Luo, C., Chen, J., and Zhou, Y.: A rapid loess flowslide triggered by irrigation in  
573 China, Landslides, 6, 55-60, 2009.  
574